Effects of pairing correlations on the neutron skin thickness and the symmetry energy

Soonchul Choi,[1] Ying Zhang,[2] Myung-Ki Cheoun,[1,*] Youngshin Kwon,[3] Kyungsik Kim,[4] and Hungchong Kim[3]
[1]*Department of Physics and OMEG Institute, Soongsil University, Seoul 06978, Korea*
[2]*Department of Physics, School of Science, Tianjin University, Tianjin 300072, China*
[3]*Research Institute of Basic Science, Korea Aerospace University, Goyang 412-791, Korea*
[4]*School of Liberal Arts and Science, Korea Aerospace University, Goyang 412-791, Korea*
(Received 10 April 2017; revised manuscript received 20 June 2017; published 18 August 2017)

We investigated effects of pairing correlations on the neutron skin thickness and the symmetry energy of finite nuclei. In this calculation we used Hartree-Fock-Bogoliubov method with Skyrme forces and effective pairing interactions. The results have been compared with available experimental data, Hartree-Fock results as well as the predictions by droplet model. Finally, our discussion was extended to study of the pairing interaction in nuclear matter. Roles of isospin $T = 0$ pairing in the nuclear matter were also discussed.

DOI: 10.1103/PhysRevC.96.024311

I. INTRODUCTION

Study of symmetry energy and its density dependence becomes a great interesting topic in nuclear physics and astrophysics. Its importance emerges out of understanding the structure of neutron-rich nuclei, various observational data of neutron stars, and recent heavy ion collision data because the isospin and density dependence of the equation of state (EoS) in nuclear matter can be characterized by the symmetry energy [1]. The nuclear EoS, which explicates the energy per nucleon of asymmetric nuclear matter, can be expanded as a function of neutron-proton asymmetry, $\delta = (\rho_n - \rho_p)/\rho$, at a given density ρ

$$\mathcal{E}(\rho,\delta) = \mathcal{E}(\rho,0) + \mathcal{E}_{\rm sym}(\rho)\delta^2 + \cdots . \tag{1}$$

The coefficient of the quadratic in Eq. (1) is the nuclear symmetry energy that can be approximated to the energy difference between the pure neutron matter (PNM) and symmetric nuclear matter (SNM) [2]. Since most of the nuclear models available these days are adjusted to the data of the binding energy of finite nuclei, they agree on the value of the symmetry energy around saturation density ρ_0. However, when it comes to its density dependence, there is a strong model dependence. In order to characterize the density dependence, one explores the symmetry energy around the saturation density, expanding it with respect to the density $x = (\rho - \rho_0)/(3\rho_0)$:

$$\mathcal{E}_{\rm sym} = J + Lx + \tfrac{1}{2}K_{\rm sym}x^2 + \cdots , \tag{2}$$

where L and $K_{\rm sym}$ are the slope and the curvature parameters of the nuclear symmetry energy at ρ_0. The leading term, J, indicates the symmetry energy at ρ_0 which values are predicted in the order of $30 \sim 35$ MeV. The second coefficient is the slope parameter defined as

$$L = 3\rho_0 \frac{\partial \mathcal{E}_{\rm sym}(\rho)}{\partial \rho}|_{\rho=\rho_0}, \tag{3}$$

but it still has a wide ambiguity ($20 \sim 100$ MeV) [3]. Since nuclear pressure can be calculated as $P(\rho,\delta) = \rho^2 d\mathcal{E}(\rho,\delta)/d\rho$, the L is proportional to the PNM pressure evaluated at saturation density ρ_0,

$$P(\rho = \rho_0, \delta = 1) = 3\rho_0 L. \tag{4}$$

Another simple parametrization of the symmetry energy is usually introduced in the interpretation of heavy ion collision data

$$\mathcal{E}_{\rm sym} \simeq \mathcal{E}_{\rm sym}(\rho_0)\left(\frac{\rho}{\rho_0}\right)^{\gamma} = J(1+3x)^{\gamma}, \tag{5}$$

from which the slope and the curvature can be represented as $L = 3J\gamma$ and $K_{\rm sym} = 9J\gamma(\gamma - 1)$ [4,5]. Many of nuclear experiments have been conducted to make a constraint on the density dependence of the symmetry energy. The parameter $\gamma = 0.4$–1.05 ($L = 88 \pm 25$ MeV) is constrained by the isospin diffusion data in heavy-ion collisions [4], while $\gamma = 0.69$ ($L \sim 65$ MeV) is deduced from isotope ratios [5]. Recent analysis by Ref. [3] shows $\gamma = 0.79 \pm 0.25$ ($L = 75 \pm 25$ MeV). But the relation is claimed not to be reliable enough because it does not properly map self-consistent results [6]. Discussion of nuclear collective motions can also give a unique chance to determine the incompressibility of the nuclear system, which is strongly related to the symmetry energy [7–12]. For instance, the giant dipole resonance in heavy nuclei reflects the value of $\gamma = 0.5$–0.65 [13], and the Thomas-Fermi model results in $\gamma = 0.51$ [14]. Although the substantial progress has been made theoretically and experimentally, the density dependence of the symmetry energy still remains uncertain and more accurate information is required to understand it.

Recently it has been regarded that the neutron skin thickness (NST), defined by the difference of the root-mean-square (rms) radii of protons and neutrons, is a conceivable clue for the symmetry energy [15–18]

$$\Delta r_{np} = \sqrt{\langle r_n^2 \rangle} - \sqrt{\langle r_p^2 \rangle}. \tag{6}$$

The NST depends on the pressure of EoS in nuclear matter, and thus is related to the first derivative of the symmetry energy like the slop parameter, L [15,19]. It can be extracted through the antiprotonic measurements [20], the parity-violating electron

*Corresponding author: cheoun@ssu.ac.kr

 ©2017 American Physical Society

scattering [21–25], the polarized proton elastic scattering [23], and other probes like α or pions which can measure electric dipole strength functions through electric dipole polarizability and/or pygmy dipole resonances [24]. Neutrino-nucleus scattering in recent neutrino beam facilities could also be an alternative study for the NST [26].

It is noticeable that the formation of the neutron skin can be affected by the pairing correlation of nucleons, which is known to have a minor effect near the saturation density $\rho \approx \rho_0$. However, in the surface of finite nuclei where the densities become lower than the saturation density due to the smearing of Fermi surface, the contribution of the pairing correlations is no longer negligible [7]. In particular, the unlike neutron-proton (np) pairing as well as the like pairing correlations by the neutron-neutron and proton-proton should also be considered for a proper account of the symmetry energy because the np pairing has isoscalar ($T = 0$) and isovector ($T = 1$) pairing components and they may have different quenching properties inside nuclei discovered in Ref. [27]. These properties should be taken into account in the mean-field description of finite nuclei, in particular, $N = Z$ isoscalar nuclei [28,29]. Even in the droplet model, the mass excesses of $N = Z$ nuclei show a zigzag dependence on the mass number due to the pairing correlations [30]. It is thus worthwhile to discuss the effects of pairing correlation on the NST and the symmetry energy in finite nuclei as well as nuclear matter.

In the present work, we mainly employ the Hartree-Fock-Bogoliubov (HFB) method with Skyrme effective interactions to estimate the symmetry energy of various nuclei as a function of NST, concentrating on the influence of pairing correlations. In Sec. II, we first briefly review the definition of the symmetry energy and coefficient for finite nuclei, and its relation with the NST in the droplet model (DM). Sections III and IV are dedicated to the main calculations and results given by the mean-field models with Skyrme functionals. In Sec. V, we discuss the effect of the pairing correlations on infinite nuclear matter. Then this paper is wrapped up with a summary and conclusions in Sec. VI.

II. NEUTRON SKIN THICKNESS AND SYMMETRY ENERGY IN DROPLET MODEL

Possible correlations between the NST (Δr_{np}) and the slop of symmetry energy, L, can be inferred from the droplet model (DM) [16–18]. In this model, the NST is given by [31]

$$\Delta r_{np}^{\rm DM} = \sqrt{\frac{3}{5}}\left[t - \frac{e^2 Z}{70J}\right] + \Delta r_{np}^{sw}, \tag{7}$$

where the quantity t is a distance between the neutron and proton mean surface locations, the second term in the bracket is due to the Coulomb repulsion. The bulk contribution t is given as

$$t = \frac{3}{2} r_0 \frac{J}{Q}\frac{1}{1+x_A}(\delta - I_C) \quad \text{with} \quad x_A = \frac{9J}{4Q}A^{-1/3}, \tag{8}$$

where J is the leading term of the symmetry energy defined before, Q is the surface stiffness coefficient, which can be extracted from semi-infinite nuclear matter calculations [32,33], and $I_C = e^2 Z/(20JR)$ with $R = r_0 A^{1/3}$. The term Δr_{np}^{sw} is a correction caused by the different surface widths b_n and b_p of the neutron and proton density profiles as

$$\Delta r_{np}^{sw} = \sqrt{\frac{3}{5}}\frac{5}{2R}\left(b_n^2 - b_p^2\right), \tag{9}$$

which can be fitted as the following ansatz:

$$\Delta r_{np}^{sw} = \left(0.3\,\frac{J}{Q} + c\right)\delta, \tag{10}$$

where $c = -0.05$ or 0.07 fm is adopted in Ref. [32]. In the DM, the symmetry energy contribution to a finite nucleus with a mass A is given by [34]

$$E_{\rm sym}^{\rm DM} = a_{\rm sym}^{\rm DM}(A)\,(\delta + x_A I_C)^2 A, \tag{11}$$

where

$$a_{\rm sym}^{\rm DM}(A) = \frac{J}{1+x_A} \tag{12}$$

is the symmetry energy coefficient of the corresponding nucleus. Then, the bulk contribution t to the neutron skin can be written in terms of symmetric matter properties as follows:

$$t = \frac{3}{2} r_0 \frac{a_{\rm sym}^{\rm DM}(A)}{Q}(\delta - I_C) = \frac{2r_0}{3J}\left[J - a_{\rm sym}^{\rm DM}(A)\right]A^{1/3}(\delta - I_C). \tag{13}$$

Therefore, one can infer from Eq. (13) a linear correlation between the NST ($\Delta r_{np}^{\rm DM}$) and the symmetry energy coefficient $a_{\rm sym}^{\rm DM}(A)$ for an isotopic chain with different mass number A as shown later on. For a given mass number A, e.g., ^{208}Pb, it is found universally in the mean-field calculation that the symmetry energy coefficient $a_{\rm sym}^{\rm DM}(A)$ equals the value of $\mathcal{E}_{\rm sym}(\rho)$ in Eq. (2) of asymmetry nuclear matter at the density $\rho = 0.1$ fm^{-3}. With this relation, one can further reduce the bulk contribution t in Eq. (13) as

$$t = \frac{2r_0}{3J} L\left[1 + x\frac{K_{\rm sym}}{2L}\right] x A^{1/3}(\delta - I_C), \tag{14}$$

which shows a linear correlation between the NST ($\Delta r_{np}^{\rm DM}$) and the slope of the symmetry energy L [16]. Not that Eq. (14) is different from the t in Ref. [16], where $\epsilon = \frac{\rho_0 - \rho}{3\rho_0}$ is used instead of $x = \frac{\rho - \rho_0}{3\rho_0}$.

Consequently, for a given nuclear force with fixed L and $K_{\rm sym}$, one could infer from Eq. (14) a linear relation between the NST (Δr_{np}) and the asymmetry parameter δ, especially for heavier nuclei. This relation is confirmed by the antiprotonic atom x-ray measurement [20], and analyzed within the droplet model, Skyrme and relativistic mean-field models [16,32], which were also used to estimate the slope of the symmetry energy L.

III. NEUTRON SKIN THICKNESS AND SYMMETRY ENERGY IN SKYRME FUNCTIONALS WITH PAIRING EFFECTS

In this section, we investigate the relation between the NST Δr_{np} in Eq. (6) and the symmetry energy $E_{\rm sym}(A)$ or the symmetry energy coefficient $a_{\rm sym}(A)$ for finite nuclei with

different mass numbers by including the effects of pairing correlations. In order to calculate the symmetry coefficient $a_{\rm sym}(A)$ for finite nuclei microscopically, we use the following recipe to rewrite the Skyrme functional in Ref. [35]:

$$\begin{aligned}\mathcal{H} &= \frac{1}{2}\hbar^2(f_n\tau_n + f_p\tau_p)\\ &+\left[\frac{t_0}{2}\left(1+\frac{x_0}{2}\right)+\frac{t_3}{12}\left(1+\frac{x_3}{2}\right)\rho^\alpha\right]\rho^2\\ &+\left[\frac{3t_1}{16}\left(1+\frac{x_1}{2}\right)-\frac{t_2}{16}\left(1+\frac{x_2}{2}\right)\right](\nabla\rho)^2\\ &-\left[\frac{t_0}{2}\left(x_0+\frac{1}{2}\right)+\frac{t_3}{12}\left(x_3+\frac{1}{2}\right)\rho^\alpha\right]\\ &\times\left(\rho_n^2+\rho_p^2\right)\\ &-\left[\frac{3t_1}{16}\left(x_1+\frac{1}{2}\right)+\frac{t_2}{16}\left(x_2+\frac{1}{2}\right)\right]\\ &\times((\nabla\rho_n)^2+(\nabla\rho_p)^2)\\ &+\frac{1}{16}\left[(t_1-t_2)\left(\mathbf{J}_n^2+\mathbf{J}_p^2\right)-(t_1x_1+t_2x_2)\mathbf{J}^2\right]\\ &+\frac{W_0}{2}\left[\mathbf{J}\cdot\nabla\rho+\mathbf{J}_n\cdot\nabla\rho_n+\mathbf{J}_p\cdot\nabla\rho_p\right]+\mathcal{H}_c, \quad (15)\end{aligned}$$

where

$$\begin{aligned}f_{n,p} &= \frac{1}{m}+\frac{1}{2\hbar^2}\left[t_1\left(1+\frac{x_1}{2}\right)+t_2\left(1+\frac{x_2}{2}\right)\right]\rho\\ &-\frac{1}{2\hbar^2}\left[t_1\left(x_1+\frac{1}{2}\right)-t_2\left(x_2+\frac{1}{2}\right)\right]\rho_{n,p}. \quad (16)\end{aligned}$$

If we assume $\rho_n=\rho_p=\frac{1}{2}\rho$ for symmetric nuclear matter, i.e.,

$$\begin{aligned}f_{n=p} &= \frac{1}{m}+\frac{1}{2\hbar^2}\left[t_1\left(1+\frac{x_1}{2}\right)+t_2\left(1+\frac{x_2}{2}\right)\right]\rho\\ &-\frac{1}{4\hbar^2}\left[t_1\left(x_1+\frac{1}{2}\right)-t_2\left(x_2+\frac{1}{2}\right)\right]\rho, \quad (17)\end{aligned}$$

the Hamiltonian is denoted as $\mathcal{H}_0$. By excluding the Coulomb energy and the spin energy in $\mathcal{H}-\mathcal{H}_0$, the density functional of the symmetry energy is given as

$$\mathcal{H}_{\rm sym}=\mathcal{H}_T+\mathcal{H}_V+\mathcal{H}_{\rm grad} \quad (18)$$

with

$$\begin{aligned}\mathcal{H}_T &= \frac{\hbar^2}{2}(f_n\tau_n+f_p\tau_p-2f_{n=p}\tau_{n=p}),\\ \mathcal{H}_V &= -\left[\frac{t_0}{4}\left(x_0+\frac{1}{2}\right)+\frac{t_3}{24}\left(x_3+\frac{1}{2}\right)\rho^\alpha\right]\rho^2\delta^2,\\ \mathcal{H}_{\rm grad} &= -\left[\frac{3t_1}{32}\left(x_1+\frac{1}{2}\right)+\frac{t_2}{32}\left(x_2+\frac{1}{2}\right)\right][\nabla(\rho\delta)]^2.\end{aligned}$$

Then the total symmetry energy $E_{\rm sym}(A)$ and the symmetry energy coefficient $a_{\rm sym}(A)$ for a finite nucleus with the mass number A are defined as

$$E_{\rm sym}(A)=\int\mathcal{H}_{\rm sym}dV=a_{\rm sym}(A)\,(\delta+x_A I_C)^2A. \quad (19)$$

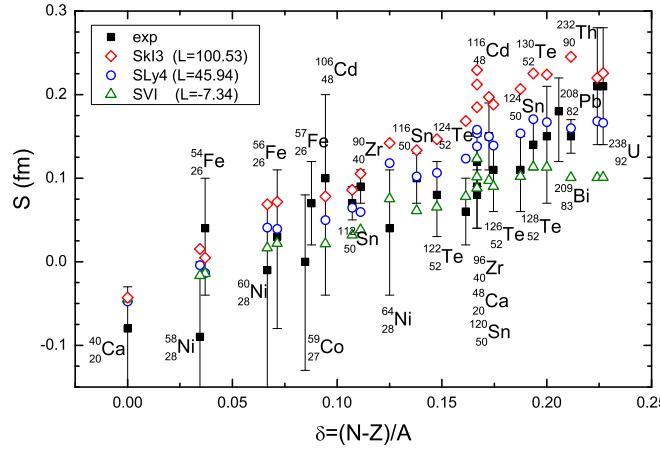

FIG. 1. Neutron skin thickness (S) calculated by the Skyrme Hartree-Fock-Bogoliubov (HFB) model with SkI3, SLy4, SVI interactions and density-dependent δ interaction (DDDI) for the pairing force, comparing with the antiprotonic measurement data [20].

Here, it should be noted that this equation is an approximation, because the symmetry energy coefficient $a_{\rm sym}(A)$ defined in DM models does not include the shell effect, while the total symmetry energy $E_{\rm sym}(A)$ includes the shell effect in the Skyrme functional. By comparison between $a_{\rm sym}(A)$ and $a_{\rm sym}^{\rm DM}(A)$, we can deduce the shell effect as shown in the numerical results in Sec. IV. In the HFB calculations, we use the box-discretized method with a box size, $R_{\rm box}=20$ fm, and the mesh size, d$r=0.1$ fm. The angular momentum cut off is taken as $l_{\rm max}=12\hbar$.

For the pairing interaction in SLy4, we use the density-dependent δ interaction (DDDI) for the like-pairing field [7,36]

$$G(\boldsymbol{r})_q=\frac{v_0}{2}\left[1-\eta\left(\frac{\rho_q(\boldsymbol{r})}{\rho_0}\right)^\alpha\right]\tilde{\rho}(\boldsymbol{r}), \quad q=n \text{ or } p, \quad (20)$$

where $\tilde{\rho}$ is the pair density. The parameters in the DDDI are taken as $v_0=-458.4$ MeV fm^3, $\eta=0.71$, $\alpha=0.59$, $\rho_0=0.08$ fm^{-3}, which are determined for the Sn isotopes [37]. The quasiparticle energy cut off is $E_{\rm cut}=60$ MeV.

In principle, one should fit the pairing strength for each employed Skyrme interaction, and also for each isotope chain according to the experimental pairing gap. But we exploit the same parameters for different Skyrme interactions in Fig. 1 in order to do systematic calculations for a large number of isotopes. This also helps us to understand the pairing effects among the selected Skyrme functionals by comparing the HF calculation without pairing to the HFB calculation with the pairing in Figs. 2–6. But, for nuclear matter, we use different parameters for SLy4 and SLy5, which are shown after Eqs. (20) and (24), respectively, because the pairing parameters are well established for nuclear matter study.

IV. NUMERICAL RESULTS OF NEUTRON SKIN THICKNESS AND SYMMETRY ENERGY

In this section, we calculate the NST (Δr_{np}) in terms of the asymmetry parameter δ, using HFB theory with three different

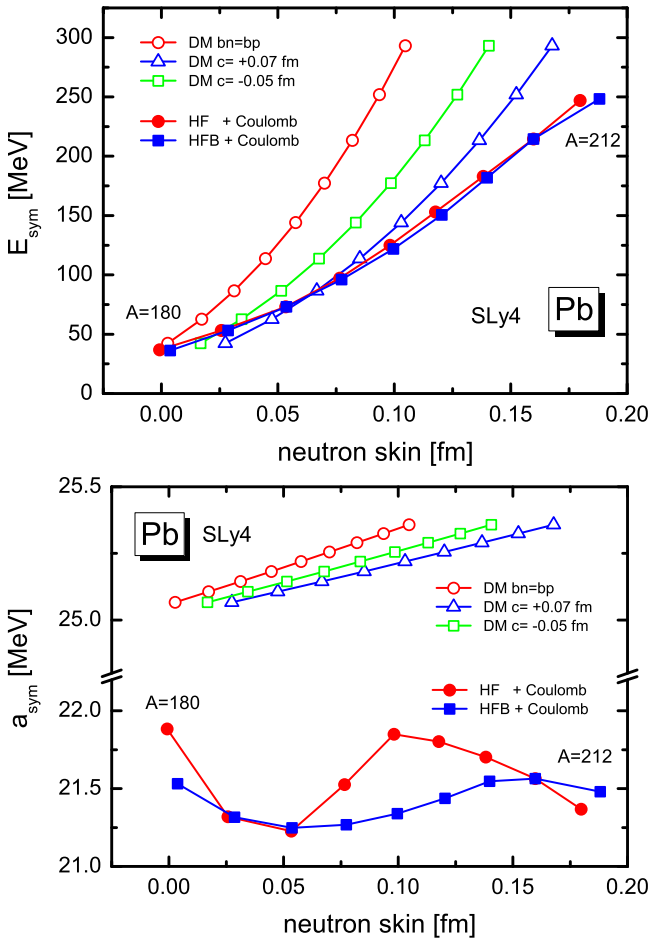

FIG. 2. Symmetry energy $E_{\rm sym}$ (upper panel) and coefficient $a_{\rm sym}$ (lower panel) as a function of NST for Pb isotopes ($A = 180,184,\ldots,212$). The filled symbols denote the results given by the Skyrme functional SLy4 of HFB calculation with (square) and HF calculation without (circle) pairing interaction. The open symbols denote the results in the droplet model (DM) without surface width corrections (circle), with the surface width correction of $c = -0.05$ fm (square) and $c = +0.07$ fm (triangle).

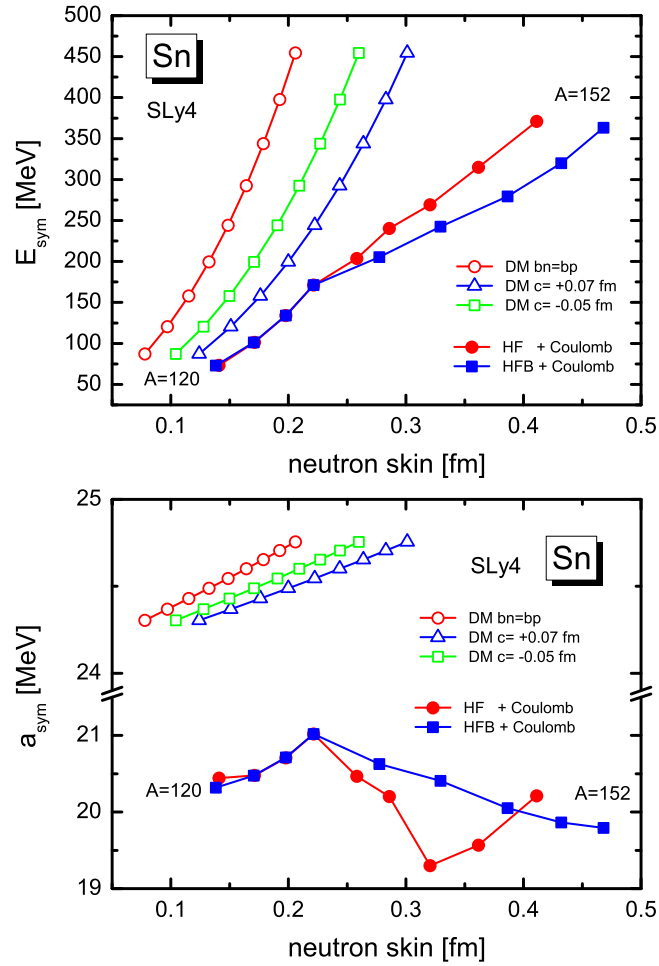

FIG. 3. Similar as Fig. 2, but for Sn isotopes with $A = 120,124,\ldots,152$.

Skyrme functionals, SkI3, SLy4, and SVI, which have quite different density dependence (characterized by L and $K_{\rm sym}$) for the symmetry energy as shown in Ref. [38]. Second, for Pb and Sn isotopes, we deduce the correlations of the NST to the symmetry energy and its coefficient only by taking SLy4 and SVI functionals which have positive and negative L values, respectively. The rms radius $\sqrt{\langle r^2_{n(p)}\rangle}$ in Eq. (6) is calculated by the self-consistent neutron (proton) density.

Figure 1 shows our results of the NST ($S = \Delta r_{np}$), as a function of $\delta = (N - Z)/A$, compared with the experimental results deduced from the antiprotonic atom x-ray data [20]. Our results are consistent with the data within uncertainties and comparable with the results in Refs. [16,32], although we include the shell and pairing effects in the full self-consistent calculations. One can see that, even if the three Skyrme functionals have quite different L and $K_{\rm sum}$, a linear relation between the NST and the asymmetry parameter δ still holds to some extent. However, the uncertainties of experimental data are still too large to deduce the L value in the present model.

Figures 2 and 3 show numerical results for the symmetry energy $E_{\rm sym}(A)$ (upper panel) and the symmetry energy coefficient $a_{\rm sym}(A)$ (lower panel) as a function of the NST for isotopic chain Pb ($A = 180,184,\ldots,212$) and Sn ($A = 120,124,\ldots,152$), respectively, calculated with the Skyrme functional SLy4. The filled circles denote the result of the Hartree-Fock results without pairing, while the filled squares stand for the result of the HFB results with the DDDI pairing. For comparison, the results from the DM calculated by Eqs. (11) and (12) are also shown in the figures by the open symbols, where the circles denote the NST without the surface width corrections, i.e., $b_n = b_p$ in Eq. (9), and the triangles (squares) denote the results given by the parametrized surface width correction with $c = +0.07$ fm ($c = -0.05$ fm). One should notice that, in our mean-field calculations, we include self-consistently the shell and pairing effects, while the DM cannot.

Taking the Pb isotopes as examples, one can see from the upper panel in Fig. 2 a large increase of the symmetry energy $E_{\rm sym}$ as a function of the NST for heavier nuclei for both the DM and mean-field calculations. The NST is known to be

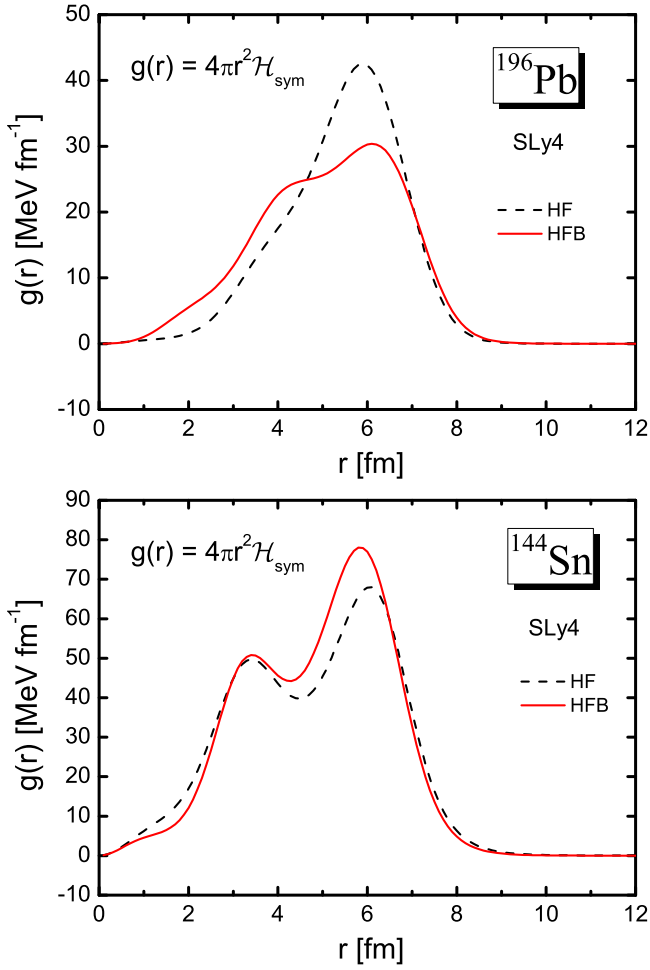

FIG. 4. Symmetry energy density distribution $g(r) = 4\pi r^2 \mathcal{H}_{\rm sym}$ in ^{196}Pb (upper panel) and ^{144}Sn (lower panel) obtained by the HF (dashed line) and HFB (solid line) calculation with SLy4 functional.

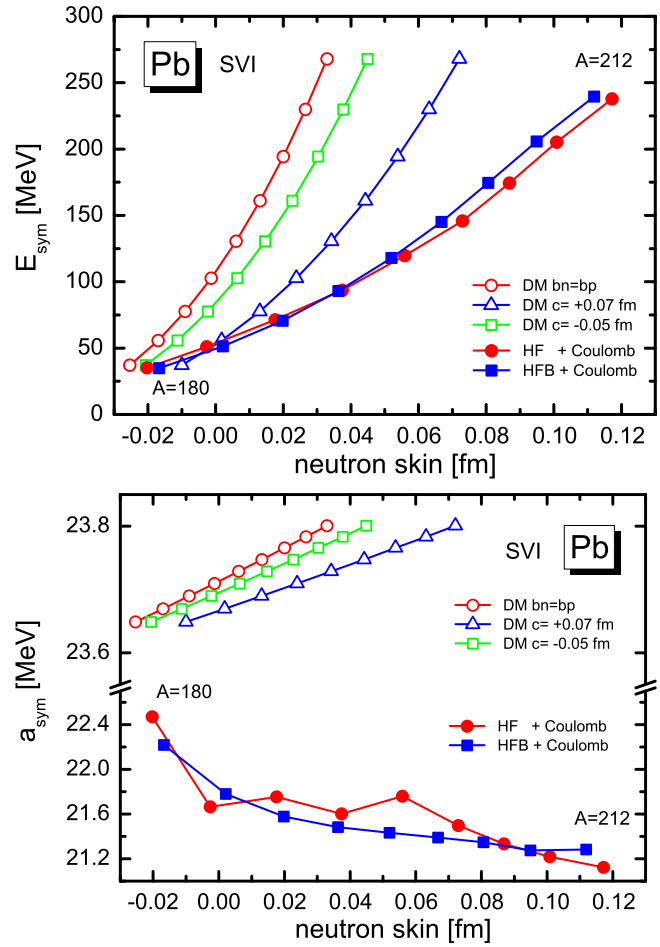

FIG. 5. Similar with Fig. 2, but calculated by the Skyrme functional SVI.

proportional to the L in the symmetry energy, which is fixed as $L = 100.53$ for SLy4 interaction. If we may measure the NST, S, one can deduce the $E_{\rm sym}$ for a given nucleus, or vice verse, from these results. Most of the symmetry energy given by the DM is larger than those given by the self-consistent mean-field calculations for a given isotope. The surface width corrections for the NST become more and more important for the heavier nuclei in the DM model.

Only for the isotope $A = 180$, the DM model without the surface width correction gives the similar results of the symmetry energy and the NST (almost zero) with the mean-field calculations. For $A = 184$, the NST of the mean-field calculation is closer to the DM result with $c = -0.05$ fm. From $A = 188$ to $A = 204$, the NST given by the mean-field model lies between the surface width correction region $c = -0.05 \sim +0.07$ fm, which is consistent with the DM ansatz in Eq. (10).

However, when it comes to the even more neutron-rich isotopes for $A = 208,212$, the mean-field calculation gives larger NST than DM. At the same time, we notice that the pairing effect from the comparison between the HF and HFB calculations is almost negligible in this example. This fact demonstrates that the larger NST in the mean-field calculations than the DM results is mainly due to the shell effects included in the HF mean field.

When we come to the symmetry energy coefficient $a_{\rm sym}$ in the lower panel in Fig. 2, the rate of change by the neutron skin is much smaller than that in $E_{\rm sym}$ because the A and δ dependence in the $E_{\rm sym}$ disappears in the coefficient $a_{\rm sym}$. In fact, the coefficient $a_{\rm sym}$ depends on the NST, but its variation is small, maximally less than 2 MeV. It means that the coefficient $a_{\rm sym}$ is a property of nuclear matter with the small contribution from the shell effect. Also we can see more clearly that the results of DM are larger than those given by the mean-field models, as explained after Eq. (19).

As expected from Eq. (13), we can see a linear increase of the symmetry energy coefficient as a function of the NST in the DM. However, this relation is not found in the mean-field model at all. It means that the NST depends on the nuclear structure of each nucleus, i.e., shell effects. Besides, the difference between the HF and HFB results in the lower panel is enlarged in the symmetry energy coefficient, $a_{\rm sym}$, with a small scale although they give the similar NST. Namely, not only the shell effects but also the pairing correlations influence the $a_{\rm sym}$ as well as the NST. For example, one can see the largest difference between the $a_{\rm sym}$ appears in the isotope $A = 196$,

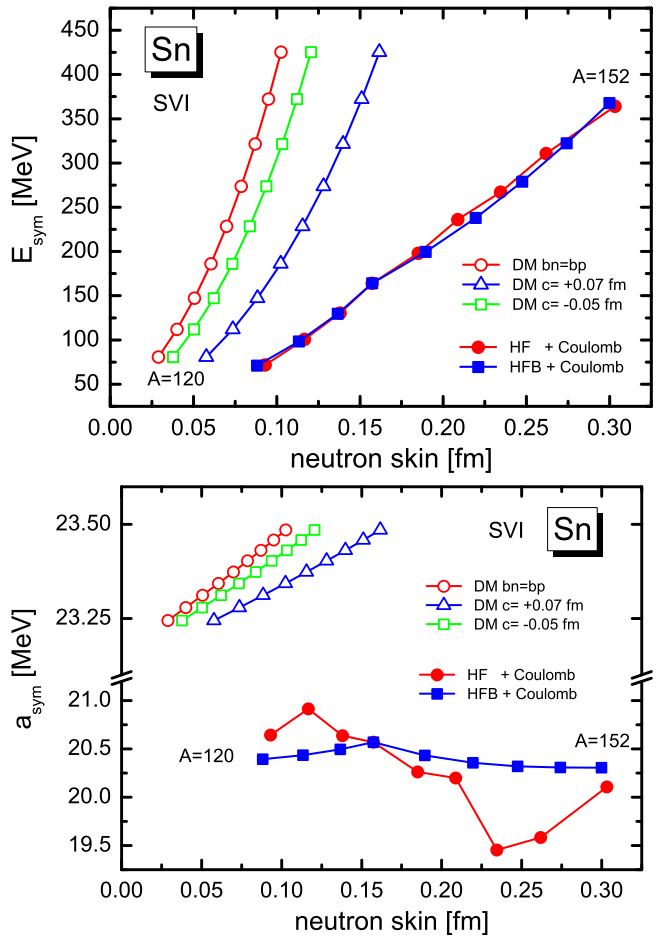

FIG. 6. Similar with Fig. 3, but calculated by the Skyrme functional SVI.

which has 114 neutrons and lies between the 82 and 126 major shells, while the smallest case appears at the double magic nucleus ($A = 208$, $N = 126$) as expected.

Figure 3 for Sn isotopes with $A = 120, 124, \ldots, 152$ shows the similar calculation results with Fig. 2 for Pb isotopes. First, one can see from the upper panel that the symmetry energy given by the DM is again systematically larger than that given by the mean-field model for a given isotope. However, the NST of all these isotopes obtained by the mean-field model is larger than those given by the DM, which is quite different from the Pb isotopes. This demonstrates that the shell effects play an important role in producing a large NST in Sn isotopes. From the comparison between the HF and HFB results, one can see that from $A = 120$ to $A = 132$, the pairing effects is almost negligible in NST. However, from $A = 136$ the pairing effects produce a larger NST for more neutron-rich nucleus, while a nucleus ($A = 132$, $N = 82$) has also no pairing interaction effects due to the double magic number.

From the lower panel in Fig. 3, we can see again, in the HFB as well as HF mean field results, that there is no linear relation like the DM between the symmetry energy coefficient and the NST in these isotopes. The largest difference between the HF and HFB results of the symmetry energy coefficient appears for the isotope $A = 144$.

In order to further understand the difference in the symmetry energy coefficient due to the pairing effect in $A = 196$, we plot the symmetry energy density $g(r) = 4\pi r^2 \mathcal{H}_{\rm sym}$ given by the HF (dashed line) and HFB (solid line) calculations in the upper panel of Fig. 4. One can see that both the symmetry energy densities by HF and HFB are mainly contributed around the surface region $r \approx 6$ fm, where the HF result without pairing is more concentrated while the HFB result with pairing is more diffusive. Integration of this distribution gives the symmetry energy, $E_{\rm sym}$. For instance, in Fig. 2, $E_{\rm sym}^{\rm HF}$ for ^{196}Pb is shown to be almost same as that by $E_{\rm sym}^{\rm HFB}$. Consequently, the tiny difference does not change the NST as shown in the x-axis label.

Similarly to the ^{196}Pb case, we plot, for ^{144}Sn, the symmetry energy density $g(r) = 4\pi r^2 H_{\rm sym}$ given by the HF (dashed line) and HFB (solid line) calculations in the lower panel of Fig. 4. One can see again that the symmetry energy densities by both HF and HFB are mainly contributed around the surface region $r \approx 6$ fm. Integration of this distribution gives rise to a bit larger symmetry energy and thus larger symmetry coefficient and NST by the HFB result than those of HF in this nucleus. This is consistent with the fact that the pairing effects become significant in open-shell nuclei, which retain a wide smearing surface region, because in open-shell nuclei the attractive short-range nucleon-nucleon force giving rise to the pairing correlations is stronger than the repulsive particle-hole force. This feature was widely discussed in other shell model and QRPA calculations [39–41].

Similar analyses are done for Pb and Sn isotopes with SVI Skyrme functional in Figs. 5 and 6. One can see that the overall behavior of the symmetry energy and coefficient are similar with those given by the SLy4. But, the NST is much smaller than those by SLy4 because the L value is much smaller than that of the SLy4 functional. However, the pairing effects produce less different NST from the HF results in these two isotope chains with the SVI functional.

From the above, we can see that the mean-field models which include self-consistently the full shell and pairing effects gives less symmetry energy and coefficient, but larger NST, compared with the DM model which does not have these two effects. In the mean-field model, the symmetry energy and coefficient are mainly contributed by the surface region, which is mainly driven by the shell and pairing effects. In particular, in open-shell nuclei, the pairing and shell effects play meaningful roles in the symmetry energy and the NST because those nuclei have wide smearing surface allowing the pairing.

V. PAIRING IN INFINITE MATTER

This section is devoted to the effects of the pairing correlations in infinite nuclear matter. Nuclear energy density for the nuclear matter can be written as a sum of Skyrme and pairing terms

$$\mathcal{E} = \mathcal{E}_{\rm Skyrme} + \mathcal{E}_{\rm pair}. \tag{21}$$

The Skyrme energy density, $\mathcal{E}_{\rm Skyrme}$, corresponds to Eq. (15), but the Coulomb, spin-orbit, and gradient terms are omitted for the case of infinite matter. In the BCS approximation as the

simplest approach, the pairing energy density is defined by

$$\mathcal{E}_{\rm pair} = -\frac{1}{2}\sum_{\tau=n,\,p} N_\tau \Delta_\tau^2, \tag{22}$$

where $N_\tau = k_{F,\tau} m_\tau^*/\pi^2\hbar^2$ is the density of neutron ($\tau = n$) and proton ($\tau = p$) states, and the pairing gap, Δ_τ, can be obtained by solving the BCS gap equation,

$$\Delta_\tau = \frac{G_\tau}{2}\int_0^{k_{F,\tau}} \frac{\Delta_\tau}{\sqrt{(\epsilon(k)_\tau - \lambda)^2 + \Delta_\tau^2}}\, dk^3. \tag{23}$$

The denominator of the integrand in Eq. (23) denotes the quasiparticle energy with the chemical potential, λ, and the single-particle energy, $\epsilon(k) = \hbar^2k^2/2m^*$, which is assumed to be the energy of free particle with the effective mass, m^*, in nuclear matter. First, we use the SLy4 functional with the density-dependent contact interaction, Eq. (20), for the pairing force used in the previous section for finite nuclei. Second, we take SLy5 functional with the pairing field, G_τ, written in the form of

$$G_\tau = v_0\left[1 - \eta\left(\frac{\rho_\tau}{\rho_0}\right)^\alpha\right]. \tag{24}$$

For nuclear matter by the SLy5, we have used two types of pairing interaction adjusting the parameter, $\eta = 0.5$ for mixed-type and $\eta = 0$ for volume-type interactions. The strength parameter v_0 for each η is determined to reproduce the pairing gap of ^{120}Sn ($\Delta \simeq 1.321$ MeV) obtained by the HFB calculation with SLy5 [42]. For SLy5, the energy cutoff for the pairing window is taken to be 60 MeV and

$$v_0 = \begin{cases} -218\ \text{MeV fm}^3 & \text{for } \eta = 0 \\ -325\ \text{MeV fm}^3 & \text{for } \eta = 0.5. \end{cases} \tag{25}$$

For simplicity, we fix the parameter α to be one since the pairing strength is rarely sensitive to it [43].

The pairing gaps obtained by self-consistently solving Eq. (23) are shown with SLy4 (upper panel) and SLy5 (lower panel) functionals in Fig. 7. The density dependence in the mixed-type interaction in SLy5 strongly suppresses the pairing gap above saturation density because of the surface-type pairing, similarly to those by SLy4 which is also a kind of mixed-type interaction due to nonzero η value. All the while, if we take the volume type pairing, the pairing gap was not suppressed in the high density region.

In fact, in contrast to the low density region where the pairing gaps are microscopically understood, there are still ambiguities at higher densities than the nuclear saturation density. Such an ultradense nuclear matter is thought to acquire superfluidity through the formation of nucleon Cooper pairs due to the dominance of the long-range attractive part of the nucleon-nucleon (NN) interaction. In this context, it may be interesting to see if the strength v_0 is far from the values constrained by finite nuclei. Then we have also tested by multiplying a factor 2 to the strength in Eqs. (20) and (25) for SLy4 and SLy5, respectively.

Moreover, recently, there are many discussions regarding the pairing correlations by the $T = 0$ channel contribution coming from the unlike pairing by the neutron-proton (np) pairing correlations [40,44–46]. The np paring has two components $T = 0$ and 1, while the like-pairing correlations from neutron-neutron and proton-proton have only $T = 1$ contribution. In particular, the $T = 0$ channel was shown to have pairing gaps much larger, about twice, than the $T = 1$ pairing channel [47,48]. That is another reason why we tested the pairing contribution on the nuclear matter case enlarged by the factor 2, whose results are presented as dashed lines in Fig. 7. The pairing gaps by the enlarged 2 v_0 become about 6 times larger than those by the standard pairing interaction.

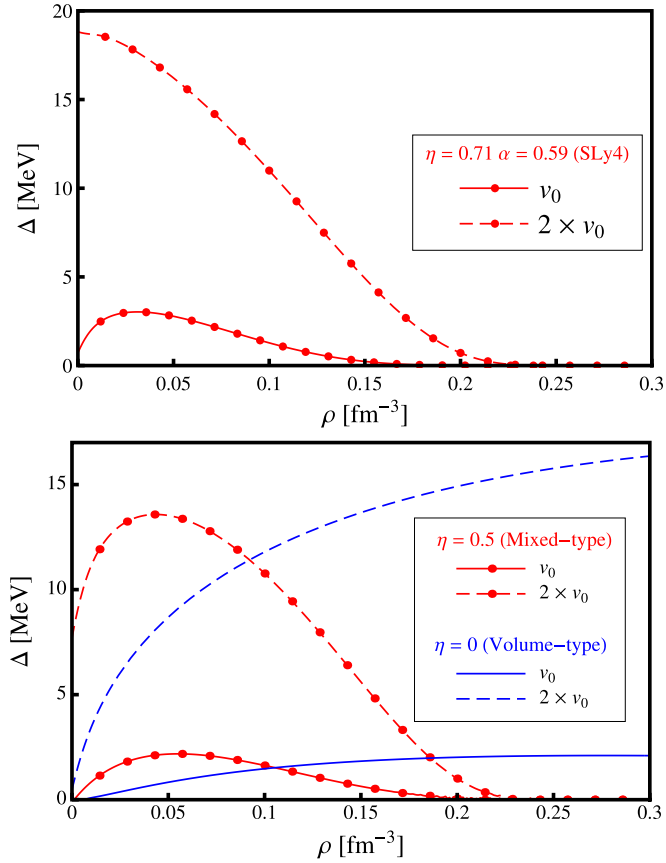

FIG. 7. Pairing gaps obtained with the density-dependent δ interaction of which parameters are determined in regard to SLy4 (upper panel) and SLy5 Skyrme (lower panel) functionals.

Finally, by using the energy functional in Eq. (21), we calculate the EoS of the system, i.e., the energy per nucleon as a function of density. The EoS of the PNM and also the SNM in the BCS approximation are shown in Fig. 8. One may notice that, in the difference between the dotted and solid lines, the pairing effects by the strength v_0 make only an indiscernible difference in the energy per nucleon, irrespective of the kinds of Skyrme functionals. Next we increase the strength parameter η twice, then the E/A becomes lower in the lower density region. Specifically, the change in the SLy4 functional makes the effect significant. But, in the high density region, the enlarged pairing gap effects appear only in the volume type interaction of SLy5. Systematic calculations involving the microscopic effects, e.g., three-body forces, detailed isospin-dependent pairing effect, etc., are required to properly describe the pairing in the nuclear matter.

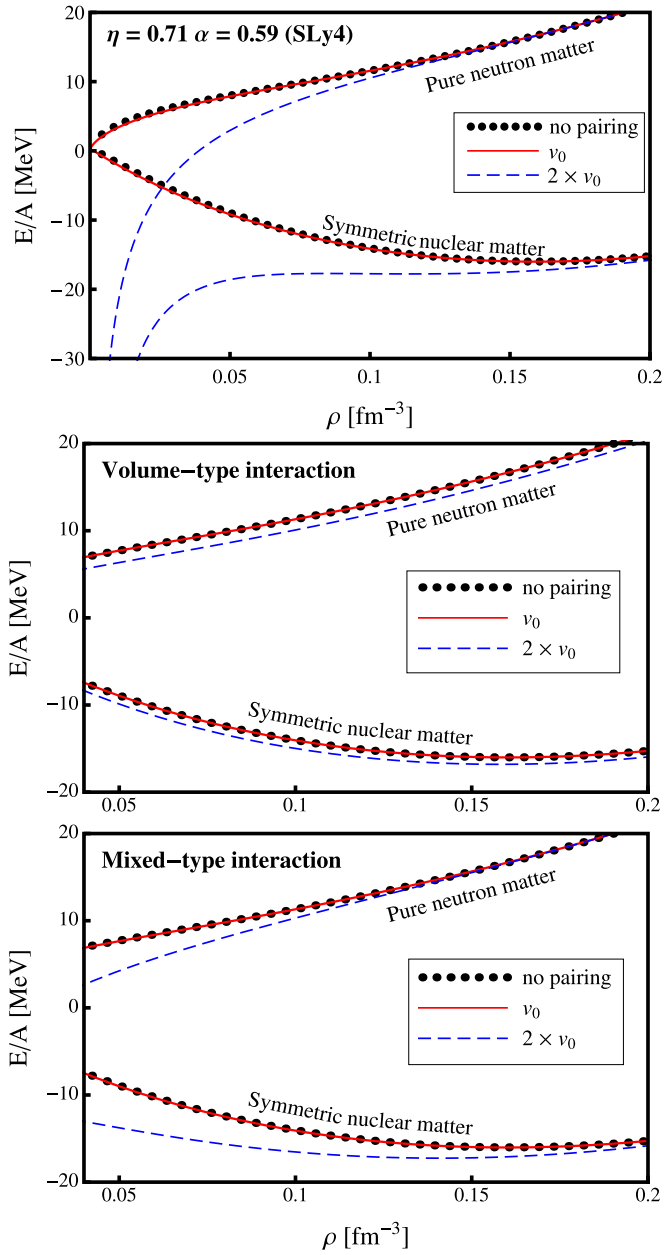

FIG. 8. Energy per nucleon versus density in symmetric nuclear and pure neutron matter for the SLy4 (upper panel) and SLy5 Skyrme (lower two panels) functionals.

VI. SUMMARY AND CONCLUSIONS

We calculated the neutron skin thickness (NST) of heavy nuclei by using a droplet model and three Skyrme functionals SLy4, SkI3, and SVI, which have quite different energy dependences, characterized by the slope L and the curvature $K_{\rm sym}$ in the symmetry energy. A linear relation between the NST and the asymmetry parameter δ can be deduced from the antiprotonic atom x-ray measurement data. Another linear relation between the NST and the L has been widely discussed. We compare our results of NST with those experimental data, which are consistent within the error bars. But it turns out to be still difficult to extract the information of the slope L from this investigation with the present experiment's accuracy, although the three different Skyrme functionals retaining different L values could reproduce the data within experimental error bars.

We also calculated the symmetry energy and its coefficient in terms of the NST for Pb and Sn isotopes from the self-consistent Skyrme models, SLy4 and SVI, and compared to those given by the droplet model. We found that most of the mean-field calculations give less symmetry energy but larger NST than those by the droplet model. The pairing effects as well as the shell structure are shown to affect more or less the neutron skin thickness. In order to argue the effects from the pairing correlation, we also compare the results between the Hartree-Fock and Hartree-Fock-Bogoliubov calculations. It turns out that the symmetry energy density is mainly distributed around the nuclear surface region and the pairing effects also show up mainly on the surface region in the symmetry energy and the NST for some open-shell nuclei having wide smearing.

By using the same Skyrme functional SLy4 used for finite nuclei and another Skyrme functional, SLy5, we calculated the pairing effects on the nuclear matter. Results by SLy4 and mixed-type SLy5 functionals show maximally about 2.5 MeV pairing gaps in the low density region. But the volume type of the pairing by SLy5 leads to about 2.5 MeV pairing gaps, which are saturated even above the normal density region. If we take into account the enlarged v_0 strength assumed to come from the $T = 0$ pairing channel, the pairing gaps were increased up to $13 \sim 19$ MeV by SLy5 and SLy4 types in the low density region, respectively. But the volume type SLy5 shows about 17 MeV pairing gap in the high density region. In the binding energy, as shown in Fig. 8, the pairing effects were not so salient for SLy5, but may become stronger by the enlarged $T = 0$ pairing correlation channel. A more stronger binding energy by this enlarged $T = 0$ pairing contribution was also confirmed for SLy4 interactions.

In conclusion, first, our results by different Skyrme functionals show that the slope of the symmetry energy, L, is a key factor for determining the NST. For example, the NST by different Skyrme functionals, which have different L values, reveals large differences as shown in the x axis in Figs. 2, 3 and 5, 6. Second, for a given symmetry energy, the NST by DM is smaller than Skyrme functionals, which comes from the shell effects considered in the mean-field calculations. Third, the pairing effects as well as the shell effects may play meaningful roles in the NST, but they are shown to be minor in the bulk properties in the symmetry energy. Nevertheless they turned out to contribute to the symmetry energy and the asymmetry coefficients of finite nuclei. As argued in the present work, the pairing effect comes mainly from the surface part. But the J, L, K in the symmetry energy are thought to be matter properties. Therefore, we addressed that the pairing interaction has to be taken into account for the NST of finite nuclei.

Finally, the $T = 0$ pairing contribution should be reexamined for a proper understanding the nuclear matter. Future experiments for the neutron skin thickness of Pb and Ca may deduce the precise constraint for the symmetry energy from those experiments. In particular, we need more detailed experimental data and more refined calculations of $T = 0$ contribution by the Skyrme functional approach for a further conclusion of the pairing effects in the nuclear matter.

ACKNOWLEDGMENTS

This work was supported by National Research Foundation of Korea under Grant Nos. NRF-2014R1A1A1038328, NRF-2014R1A2A2A05003548, and NRF-2015K2A9A1A06046598, and the National Natural Science Foundation of China under Grant No. 11405116. The work of K. S. Kim was supported by the National Research Foundation of Korea (Grant No. 2015R1A2A2A01004727)

[1] B. A. Li, L. W. Chen, and C. M. Ko, Phys. Rep. **464**, 113 (2008).
[2] I. Vidana, C. Providencia, Artur Polls, and Arnau Rios, Phys. Rev. C **80**, 045806 (2009).
[3] X. Viñas, M. Centelles, X. Roca-Maza, and M. Warda, Eur. Phys. J. A **50**, 27 (2014).
[4] M. B. Tsang, Y. Zhang, P. Danielewicz, M. Famiano, Z. Li, W. G. Lynch, and A. W. Steiner, Phys. Rev. Lett. **102**, 122701 (2009).
[5] L. W. Chen, C. M. Ko, and B. A. Li, Phys. Rev. Lett. **94**, 032701 (2005); Phys. Rev. C **72**, 064309 (2005); B. A. Li and L. W. Chen, *ibid.* **72**, 064611 (2005).
[6] J. Dong, W. Zuo, Jianzhong Gu, and U. Lombardo, Phys. Rev. C **85**, 034308 (2012).
[7] E. Khan, J. Margueron, G. Colo, K. Hagino, and H. Sagawa, Phys. Rev. C **82**, 024322 (2010).
[8] J. Piekarewicz, Phys. Rev. C **73**, 044325 (2006).
[9] A. Klimkiewicz, N. Paar, P. Adrich, M. Fallot, K. Boretzky, T. Aumann, D. Cortina-Gil, U. DattaPramanik, T. W. Elze, H. Emling, H. Geissel, M. Hellstrom, K. L. Jones, J. V. Kratz, R. Kulessa, C. Nociforo, R. Palit, H. Simon, G. Surowka, K. Summerer, D. Vretenar, and W. Walus, Phys. Rev. C **76**, 051603(R) (2007).
[10] N. Paar, D. Vretenar, and P. Ring, Phys. Rev. Lett. **94**, 182501 (2005).
[11] H. Sagawa and T. Suzuki, Phys. Rev. C **59**, 3116 (1999).
[12] V. Baran, M. Colonna, M. Di Toro, A. Croitoru, and D. Dumitru, Phys. Rev. C **88**, 044610 (2013).
[13] L. Trippa, G. Colo, and E. Vigezzi, Phys. Rev. C **77**, 061304(R) (2008).
[14] W. D. Myers and W. J. Świątecki, Nucl. Phys. A **601**, 141 (1996); Phys. Rev. C **57**, 3020 (1998).
[15] S. Typel and B. A. Brown, Phys. Rev. C **64**, 027302 (2001).
[16] M. Centelles, X. Roca-Maza, X. Viñas, and M. Warda, Phys. Rev. Lett. **102**, 122502 (2009).
[17] X. Roca-Maza, M. Centelles, X. Viñas, and M. Warda, Phys. Rev. Lett. **106**, 252501 (2011).
[18] X. Roca-Maza, M. Centelles, X. Viñas, and M. Warda, J. Phys. Conf. Ser. **321**, 012052 (2011).
[19] B. A. Brown, Phys. Rev. Lett. **85**, 5296 (2000).
[20] A. Trzcińska, J. Jastrzebski, P. Lubiński, F. J. Hartmann, R. Schmidt, T. von Egidy, and B. Kłos, Phys. Rev. Lett. **87**, 082501 (2001).
[21] C. J. Horowitz, Z. Ahmed, C. M. Jen, A. Rakhman, P. A. Souder, M. M. Dalton, N. Liyanage, K. D. Paschke, K. Saenboonruang, R. Silwal, G. B. Franklin, M. Friend, B. Quinn, K. S. Kumar, D. McNulty, L. Mercado, S. Riordan, J. Wexler, R.W. Michaels, and G. M. Urciuoli, Phys. Rev. C **85**, 032501 (2012).
[22] M. B. Tsang, J. R. Stone, F. Camera, P. Danielewicz, S. Gandolfi, K. Hebeler, C. J. Horowitz, J. Lee, W. G. Lynch, Z. Kohley, R. Lemmon, P. Moller, T. Murakami, S. Riordan, X. Roca-Maza, F. Sammarruca, A. W. Steiner, I. Vidana, and S. J. Yennello, Phys. Rev. C **86**, 015803 (2012).
[23] J. Zenihiro, H. Sakaguchi, T. Murakami, M. Yosoi, Y. Yasuda, S. Terashima, Y. Iwao, H. Takeda, M. Itoh, H. P. Yoshida, and M. Uchida, Phys. Rev. C **82**, 044611 (2010).
[24] C. Iwamoto *et al.*, Phys. Rev. Lett. **108**, 262501 (2012).
[25] K. Kim and Myung-Ki Cheoun, J. Phys. Soc. Jpn. **82**, 024201 (2013).
[26] K. Patton, J. Engel, G. C. McLaughlin, and N. Schunck, Phys. Rev. C **86**, 024612 (2012).
[27] H. Matsubara, A. Tamii, H. Nakada, T. Adachi, J. Carter, M. Dozono, H. Fujita, K. Fujita, Y. Fujita, K. Hatanaka, W. Horiuchi, M. Itoh, T. Kawabata, S. Kuroita, Y. Maeda, P. Navratil, P. vonNeumann-Cosel, R. Neveling, H. Okamura, L. Popescu, I. Poltoratska, A. Richter, B. Rubio, H. Sakaguchi, S. Sakaguchi, Y. Sakemi, Y. Sasamoto, Y. Shimbara, Y. Shimizu, F. D. Smit, K. Suda, Y. Tameshige, H. Tokieda, Y. Yamada, M. Yosoi, and J. Zenihiro, Phys. Rev. Lett. **115**, 102501 (2015).
[28] P. Ring, Prog. Part. Nucl. Phys. **37**, 193 (1996).
[29] K. Neergard, Phys. Rev. C **80**, 044313 (2009).
[30] P. Vogel, Nucl. Phys. A **662**, 148 (2000).
[31] W. Myers and W. Swiatecki, Nucl. Phys. A **336**, 267 (1980).
[32] M. Warda, X. Viñas, X. Roca-Maza, and M. Centelles, Phys. Rev. C **80**, 024316 (2009).
[33] M. Centelles, M. Del Estal, and X. Viñas, Nucl. Phys. A **635**, 193 (1998).
[34] W. Myers, *Droplet Model of Atomic Nuclei* (Plenum, New York, 1977).
[35] J. Dong, W. Zuo, and J. Gu, Phys. Rev. C **87**, 014303 (2013).
[36] Y. Zhang, Y. Chen, Jie Meng, and P. Ring, Phys. Rev. C **95**, 014316 (2017).
[37] M. Matsuo, Y. Serizawa, and K. Mizuyama, Nucl. Phys. A **788**, 307c (2007).
[38] M. Dutra, O. Lourenco, J. S. Sa Martins, A. Delfino, J. R. Stone, and P. D. Stevenson, Phys. Rev. C **85**, 035201 (2012).
[39] E. Ha, M. K. Cheoun, and F. Šimkovic, Phys. Rev. C **92**, 044315 (2015).
[40] E. Ha and Myung-Ki Cheoun, Phys. Rev. C **94**, 054320 (2016).
[41] E. Ha and Myung-Ki Cheoun, Euro. Phys. J. A **53**, 26 (2017).
[42] L. G. Cao, H. Sagawa, and G. Colo, Phys. Rev. C **86**, 054313 (2012).
[43] J. Dobaczewski, W. Nazarewicz, and P. G. Reinhard, Nucl. Phys. A **693**, 361 (2001).
[44] A. Gezerlis, G. F. Bertsch, and Y. L. Luo, Phys. Rev. Lett. **106**, 252502 (2011).
[45] H. Sagawa, C. L. Bai, and G. Colo, Phys. Scr. **91**, 083011 (2016).
[46] S. Frauendorf and A. O. Miacchiavelli, Prog. Part. Nucl. Phys. **78**, 24 (2014).
[47] E. Garrido, P. Sarriguren, E. Moya de Guerra, and P. Schuck, Phys. Rev. C **60**, 064312 (1999).
[48] E. Garrido, P. Sarriguren, E. Moya de Guerra, U. Lombardo, P. Schuck, and H. J. Schulze, Phys. Rev. C **63**, 037304 (2001).